Energy 141 (2017) 1038–1051

Contents lists available at ScienceDirect

Energy

journal homepage: www.elsevier.com/locate/energy

Dynamic control strategy of a distillation system for a composition-adjustable organic Rankine cycle

Enhua Wang [a, b], Zhibin Yu [b, *], Peter Collings [b]

[a] School of Mechanical Engineering, Beijing Institute of Technology, Beijing 100081, China
[b] School of Engineering, University of Glasgow, Glasgow G12 8QQ, UK

ARTICLE INFO

Article history:
Received 11 May 2017
Received in revised form
11 September 2017
Accepted 28 September 2017
Available online 30 September 2017

Keywords:
Organic Rankine cycle
Zeotropic mixture
Distillation column
Dynamic composition control
Response time

ABSTRACT

Using zeotropic mixtures as working fluids can improve the thermal efficiency of Organic Rankine cycle (ORC) power plants for utilising geothermal energy. However, currently, such ORC systems cannot regulate the composition of zeotropic mixtures when their operating conditions change. A composition-adjustable ORC system could potentially improve the thermal efficiency by closely matching the cycle to the changing ambient conditions provided that the composition of the working fluid mixture can be adjusted in an economic way. In this paper, a dynamic composition control strategy has been proposed and analysed for such a composition-adjustable ORC system. This method employs a distillation column to separate the two components of the mixture, which can then be pumped back to the main ORC system to adjust the composition of the zeotropic mixture to the required level according to the ambient temperature. The dynamic composition control strategy is simulated using an optimisation algorithm. The design method of the distillation column is presented and its dynamic response characteristics have been analysed using Aspen Plus Dynamics. The results indicate that the average power output can be significantly improved using a composition-adjustable ORC system when the ambient temperature decreases. The size of the distillation system is relatively small and its energy (mainly thermal) consumption is only around 1% of the system's input heat. The research results also show that the dynamic response characteristics of the distillation system can satisfy the requirements of the ORC system.

1. Introduction

Low-temperature heat energy sources are abundant globally, but are largely underutilised at present. For instance, a huge amount of geothermal energy sources are available in the temperature range between 80 and 120 °C [1,2]. The organic Rankine cycle (ORC) is a promising technology for power generation from such low-temperature heat sources. Although the market for ORC power generation equipment is growing rapidly, the installed capacity of ORC systems is still very low so far. One of the barriers is their relatively low thermal efficiency, and consequently a long payback period. Therefore, it is critical to improve the thermal efficiency of ORC power plants to facilitate their uptake.

When a zeotropic mixture is used as the working fluid for an ORC system, it differs from pure working fluids which stay at a constant temperature during their phase changing processes, in that a temperature glide will take place during the evaporation and condensation processes, which can enhance the level of temperature profile match in the heat exchangers such as evaporators and condensers [3]. Considerable efforts have been made to study ORC systems using zeotropic mixtures as working fluids. In the 1990s, a theoretical analysis by Angelino et al. indicated that using zeotropic mixtures as working fluids could improve the thermal efficiency of an ORC [4]. Aiming at low-temperature geothermal power generation, Habka and Ajib revealed that a zeotropic mixture is better than the corresponding pure fluids [5]. Kang analysed the performance of an ORC with 10 binary mixtures of HFC/HC and HFO/HC [6]. The results indicated that the maximum net power output corresponding to an optimal mixture composition with a highest temperature glide. Radulovic et al. studied the effect of composition variation of mixtures R143a/R124 and R143a/RC318 on the system performance of a supercritical ORC and the cycle efficiency could be improved by 15% in comparison with pure R143a [7]. Yang et al. analysed eight different zeotropic mixtures for ORC systems to recover energy from the waste heat carried by the exhaust gases of an internal combustion engine and R145b showed a maximum

* Corresponding author.
E-mail address: Zhibin.Yu@glasgow.ac.uk (Z. Yu).

https://doi.org/10.1016/j.energy.2017.09.141

exergy efficiency of 39.88% [8]. Li et al. studied the performance of an ORC using a zeotropic mixture as working fluid for energy recovery from industrial flue gases. It is found that the thermal efficiency could be improved if a suitable composition is chosen, but one drawback was that the heat transfer areas of the evaporator and the condenser had to be increased [9]. Chaitanya et al. investigated the thermodynamic performance of an ORC with ternary alkane mixtures for small solar power generation applications. The results indicated that zeotropic mixtures could improve the system's efficiency and reduce its expander size [10].

For an ORC system using a zeotropic mixture as working fluid, the optimal composition corresponding to the maximum thermal efficiency strongly depends on the temperature of heat source [11,12]. A research by Chys et al. showed that a better performance could be obtained with a zeotropic mixture when the heat source temperature is relatively lower [13]. Harvig et al. reported that the selection of the optimal composition must ensure the critical temperature of the zeotropic mixture is around 30–50 °C below the heat source temperature. Furthermore, the temperature glide in the condenser should be close to the temperature increment of the cooling fluid [14]. Using a suitable zeotropic mixture with an optimal composition is critical for optimising an ORC system. If a zeotropic mixture is selected improperly, the system performance may be even lower than that of the ORC system using the corresponding pure working fluids [15,16].

Since a huge amount of geothermal energy exists with a relatively low temperature, it is important to comprehensively evaluate the feasibility of using zeotropic mixtures for low-temperature geothermal power plants. So far, most of investigations indicated that using zeotropic mixtures could improve the system performance of ORC systems. Desideri and Bidini compared an ORC system with conventional single flash/binary flash power plant and reported that using ORC could harness geothermal energy more efficiently [17]. To improve degree of match of temperature profiles within the evaporator and condenser of a geothermal ORC system, Yue et al. used a zeotropic mixture of isobutane and isopentane as working fluid and the system's thermal efficiency was improved [18]. For a heat source with a temperature below 120 °C, Heberle et al. reported that the system efficiency could potentially be improved by 15% using isobutane/isopentane and R227ea/R245fa as working fluids, instead of pure working fluids [19]. Another investigation for low-temperature geothermal power plants by Liu et al. also showed that an ORC power plant using a mixture of isobutane and isopentane could produce 4–11% more power than using pure isobutane [20].

It is therefore important to further explore methods that can improve the efficiency of ORCs using zeotropic mixtures as working fluids. Andreasen et al. proposed a split evaporation concept for low-grade heat sources. A separator is installed at the outlet of the recuperator to improve the boiling process [21]. Liu et al. discussed the effect of temperature glide during the condensing process and found that such a temperature glide should be matched with the temperature profile of the cooling fluid [22]. Li et al. used a liquid-separated condenser for an ORC using a zeotropic mixture of R600/R601a [23]. It is reported that this method could improve the heat transfer coefficient of the condenser evidently. Thus, the area and cost of the condenser using zeotropic mixture can be decreased significantly.

On the other hand, various optimisation algorithms were employed for simulating different ORC systems [24,25]. To maximise the thermal efficiency, Victor et al. used a simulated annealing algorithm to calculate the optimal composition of zeotropic mixture [26]. Based on a multi-objective optimisation method, a series multi-stage ORC system was found to be better than a parallel multi-stage ORC system when zeotropic mixtures were used as working fluids [27–29]. However, once the optimal composition is determined, the above-mentioned methods cannot alter it during the operation.

For a conventional geothermal power plant, the design point is normally selected according to the maximum ambient temperature in summer. However, the ambient temperature changes with time and seasons, leading to a variation in the exergy of the geothermal brine. Collings et al. proposed a method to tune the composition of an air-cooled ORC system according to the ambient temperature using a distillation system, but the model and detailed simulation of the distillation were not provided [30]. Wang et al. studied the performance of a Kalina cycle using a separator to adjust the composition of ammonia-water mixture [31]. Both methods indicated that the annual average thermal efficiency could be significantly improved. However, these investigations did not consider the dynamic response time during the composition tuning operation. Response time is the time that a system takes to react to a given input. The composition of zeotropic mixture must be adjusted in response to the ambient temperature. If the dynamic response time of the composition tuning system is larger than the variation time of the ambient temperature, the practical composition value of the zeotropic mixture will deviate from the optimal value and thus the system performance will be deteriorated. Moreover, the optimal size of the distillation system and its power consumption remain unknown, and thus further investigation is needed.

In this paper, the energy efficiency of a composition-adjustable ORC with a distillation system is analysed using a steady state optimisation code. A dynamic composition control strategy is then proposed to compute the time needed for the required composition adjustment. Based on this strategy, a design method for the distillation system is presented using Aspen Plus. Finally, a dynamic model of the distillation system is developed using Aspen Plus Dynamics to study the dynamic response time. The results show that the average efficiency of the design ORC system can be improved significantly. Meanwhile, the designed composition control strategy can regulate the composition according to the changing ambient temperature and the response time of the distillation system can satisfy the requirements.

2. Operation principle of composition adjusting

The ORC system studied in this paper uses a zeotropic mixture for power generation from low temperature geothermal energy. Most zeotropic mixtures used for an ORC system are low boiling point alkanes or HFCs. Among these working fluids, a zeotropic mixture consisting of R134a and R245fa is considered suitable for low-temperature geothermal heat sources [30,32]. Therefore, R134a and R245fa are used in this study and their thermodynamic properties are listed in Table 1.

Fig. 1 shows a T-x (i.e., temperature − mass fraction) diagram of zeotropic mixture composed of R134a and R245fa under an example pressure of 1.4 MPa. For the designed composition-

Table 1
Properties of the working fluids.

Substance	Molecular mass [kg/kmol]	T_b [a] [K]	P_{cr} [b] [Mpa]	T_{cr} [c] [K]
R245fa	134.05	288.05	3.64	427.2
R134a	102.03	247.08	4.06	374.2
Water	18.02	373.12	22.06	647.1
Ammonia	17.03	239.82	11.33	405.4

[a] T_b: normal boiling point.
[b] P_{cr}: critical pressure.
[c] T_{cr}: critical temperature.

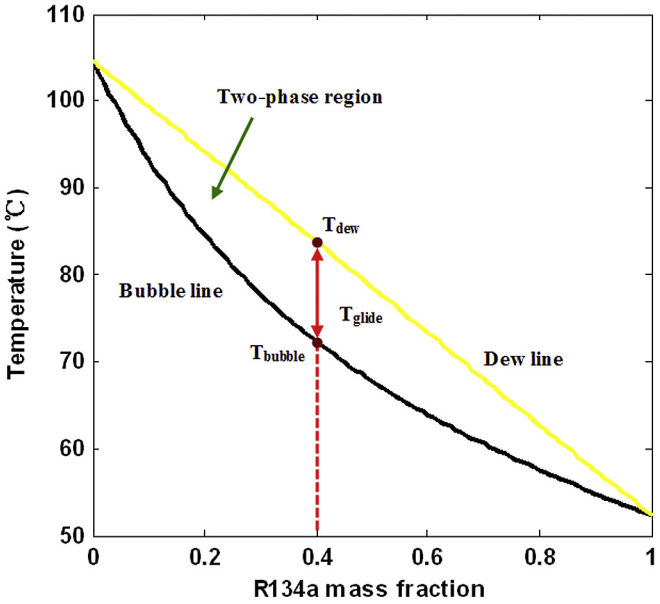

Fig. 1. Dew and bubble lines of an R134a-R245fa zeotropic mixture.

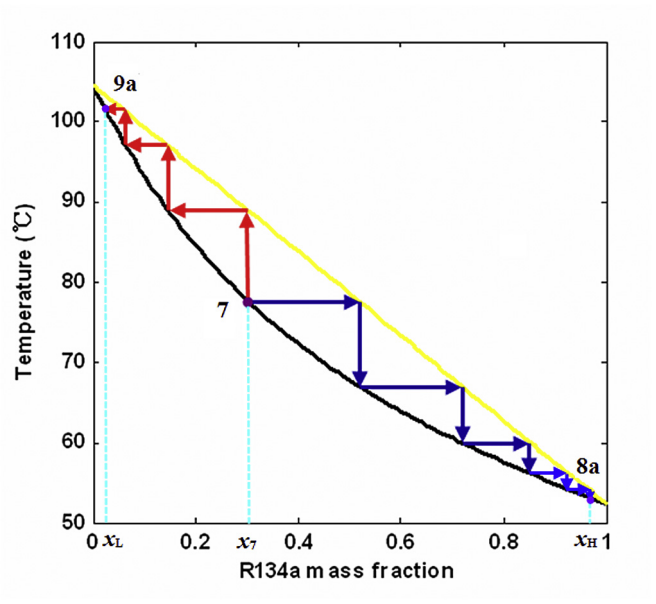

Fig. 2. Distillation process of a zeotropic mixture.

adjustable ORC, the condensation pressure is constant while the evaporation pressure varies. It can be seen that the temperature glide between the bubble and dew lines is much smaller than that of ammonia/water mixture used in Kalina cycle (see Fig. 3 in Ref. [31]). For instance, it is only 11.6 °C when the mass fraction of R134a in the mixture is 0.4. Therefore, it is unsuitable to use a separator like the Kalina cycle to adjust the working fluid composition for the ORC with zeotropic mixture R134a/R245fa. Instead, a distillation system is used to separate these two components with different boiling points.

Industrial distillation is normally performed in a vertical cylindrical column known as distillation column with several trays inside. The feed is supplied to the middle of the column. Due to the different volatility of the components in the zeotropic mixture, the distillation process separates the components by selective evaporation and condensation. The “lightest” product with the lowest boiling point exits from the top of the column and the “heaviest” product with the highest boiling point exits from the bottom of the column. More details of binary distillation process can be found in Ref. [33].

Herein, the distillation process is illustrated in Fig. 2. The mass fraction of R134a in Stream 7 is represented by x_7. The saturated liquid state at the inlet of the distillation column is denoted by Point 7. In the distillation column, equilibrium between liquid and gas mixtures under different temperatures occurs at each stage. At the top of the distillation column, Stream 8a with an R134a mass fraction of x_H is produced. At the bottom, Stream 9a contains an R134a mass fraction of x_L.

As shown in Fig. 3, differing from a conventional ORC system, it has a composition control subsystem that can adjust the composition of working fluid mixture within the ORC cycle in situ. The composition control system consists of Pump 2, Tank 2, Distillation Column, Valve 1 and Valve 2, Tank 3, Tank 4, Pump 3, and Pump 4.

Pump 1 extracts the zeotropic mixture from the condenser and pressurises it to the evaporating pressure. The mixture absorbs heat energy from geothermal brine in the evaporator and turns into high-pressure vapor. After expanding in the turbine to produce power, it condenses in the air-cooled condenser and turns into saturated liquid that flows into Tank 1. The composition control system can adjust the composition of the zeotropic mixture according to the ambient temperature. First, the composition control strategy calculates the required mass flow rate of Stream 6a that Pump 2 draws out from Tank 1 to Tank 2. The working fluid accumulates in Tank 2 for a fixed period of time. Pump 3 then delivers a certain amount of working fluid as determined by the composition control strategy to the distillation column. At its outlets, the zeotropic mixture is separated into two streams. Stream 8 contains high-purity low boiling point fluid (i.e., R134a), while Stream 9 contains high-purity high boiling point fluid (i.e., R245fa). These two streams flow to Tanks 3 and 4, respectively. In the meantime, the composition control strategy also determines the required mass flow rates of Steams 10 and 11. Then, Pumps 4 and 5 pump the corresponding mass flow rates to the mixer to compensate the working fluid mixture that has been extracted from the ORC power system. Valves 1 and 2 are used to control the mass flow rates at the outlets of the distillation column (see Section 5.2). In this way, the composition of the working fluid mixture in the ORC can be regulated. A density sensor installed at the inlet of Pump 1 can monitor the density of the zeotropic mixture. Based on the measured density, working pressure, and temperature, the composition can be determined.

Since the proposed composition-adjustable ORC system is developed for utilising low-temperature heat sources, the working temperature inside the reboiler of the distillation column may be higher than that of the heat source. In these particular cases, the reboiler may be heated using other heat sources. In this study, the energy consumption of the reboiler is evaluated in Section 5.

Once the system is designed and built, the size of the turbine and the heat transfer area of all the heat exchangers are fixed. The composition of the working fluid is adjusted by the distillation system. The operating pressure at the inlet of the turbine is regulated by the mass flow of Pump 1 and the load to the turbine. The operating temperature at the outlet of the condenser is controlled by the mass flow of the fans. Unlike the theoretical analysis in this paper, in practice, the system operation conditions may differ from the optimal points, and therefore the entire control system should regulate the above relevant parameters accordingly. In addition, monitoring and protection systems will normally be designed to avoid potential damages under some abnormal operation conditions.

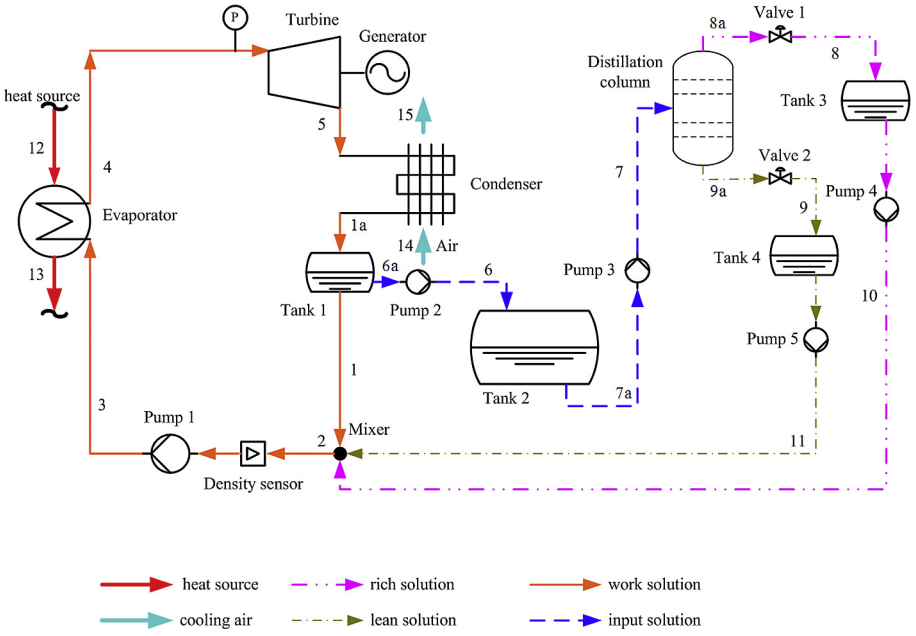

Fig. 3. Schematic of a composition-adjustable ORC system with a composition tuning.

The main working processes of the composition-adjustable ORC system are shown in Fig. 4. The blue and green dashed lines represent the bubble and dew lines at the high/low pressure side, respectively. The magenta solid lines denote the main working process of the ORC system 1-2-3-4-1. For the zeotropic mixture, the temperatures of the evaporating process 2–3 and the condensing process 4-1 are not constant. Processes 7–8 and 7–9 corresponds the distillation process. In fact, it should be denoted by a series of stepped lines similar like that in Fig. 2. Here, they are simplified by two red dashed lines. The mixing process in the mixer is depicted by 10-2′, 11-2′, and 2-2'. State 2′ represents the state at the outlet of Pump 1 for the next cycling where the composition of the working fluid may be changed.

The operation principle of the designed composition-adjustable ORC system can be explained in Fig. 5. The turbine is assumed to be able to operate at variable pressure ratio with a constant efficiency. When the ambient temperature is at a medium value, Point A represents the working state of the zeotropic mixture at the outlet of the air-cooled condenser, which is constrained by the pinch point temperature difference (PPTD) in the condenser. On the other hand, the temperature of the zeotropic mixture at the outlet of the evaporator is fixed at T_4. The corresponding state is shown as Point D. If the ambient temperature drops, the mass fraction of R134a has to be increased. Point A shifts to Point B to keep the PPTD of the condenser unchanged. Accordingly, Point D moves to Point E to keep the temperature at the outlet of the evaporator at T_4. Consequently, the working pressure at Point E is now greater than that of Point D, which can be controlled by Pump 1. If the ambient temperature rises, the mass fraction of R134a will be reduced so the

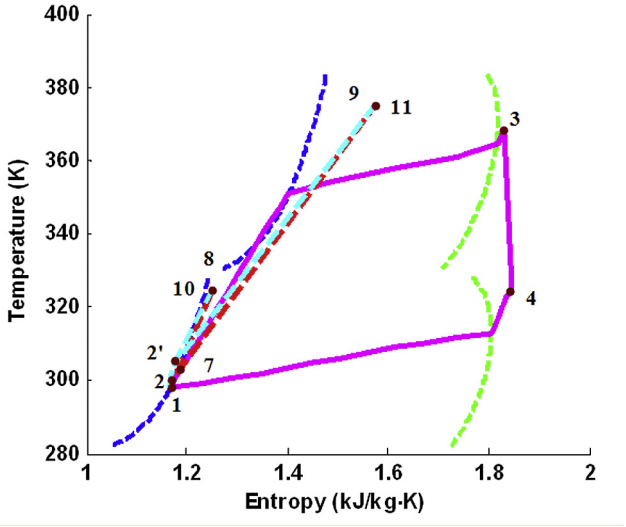

Fig. 4. A simplified T-s diagram of the composition-adjustable ORC system.

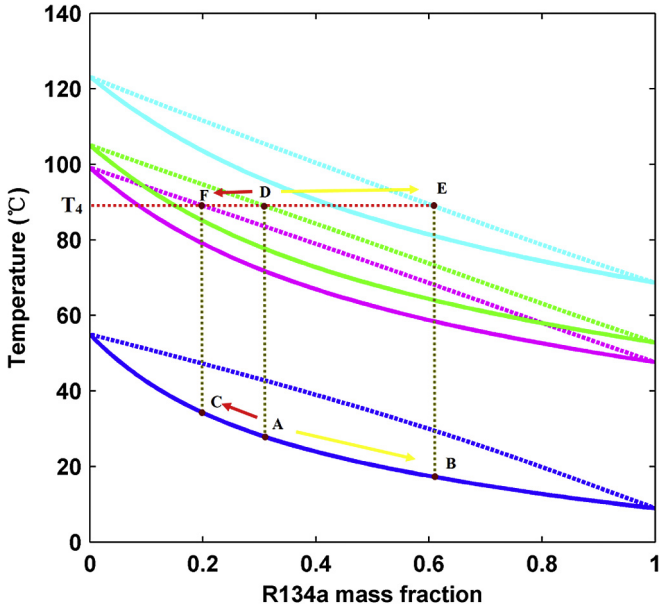

Fig. 5. Working principle of the composition-adjustable ORC system.

working Point A will shift to Point C. The corresponding Point D will be changed to Point F by decreasing the output pressure of Pump 1. In summary, the condensation pressure of the zeotropic mixture keeps constant when the composition is regulated in response to the ambient temperature. Thus, the working fluid temperature at the outlet of the air-cooled condenser can be controlled. As the working fluid temperature at the outlet of the evaporator is limited by the heat source temperature, the evaporation pressure must be changed accordingly to keep the working fluid in a gaseous state. Therefore, the exergy efficiency of the ORC system as described above can be maximised by adjusting the pressure at the outlet of Pump 1 when the ambient temperature decreases.

According to the working principle of the composition-adjustable ORC system, the condensation pressure of the zeotropic mixture should be greater than the ambient pressure to avoid air leaks into the ORC system. For a certain condensation pressure, the temperature range of the zeotropic mixture at the bubble line must match the variation range of the ambient temperature. On the other hand, the corresponding evaporation pressure of the zeotropic mixture should not be too high for safety. In addition, ideally, the zeotropic mixture should be not toxic, none-flammable, and cheap; and should have zero ODP and low GWP.

3. Improvement of energy efficiency

In this section, the improvement of energy efficiency by using composition adjustment is evaluated using a thermodynamic analysis method. The relationship between the optimal composition and the ambient temperature is obtained. In this analysis, the temperature of the geothermal brine is set to 100 °C as a case study. A thermodynamic model similar to that of reference [31] is firstly developed in Matlab for the ORC system. The flow resistance and heat loss in the pipes are neglected to simplify the model. The operation pressure of the air-cooled condenser is set to 0.4 MPa. The saturated liquid state at the outlet of the condenser is specified based on the ambient temperature

$$T_1 = T_a + 10. \tag{1}$$

The corresponding air temperature at the other outlet of the condenser is determined using a pinch-point analysis method.

The working fluid temperature at the outlet of the evaporator is set to

$$T_4 = T_{hs} - 5. \tag{2}$$

Accordingly, the working fluid temperature at the inlet of the evaporator can be obtained using a pinch-point analysis method.

The corresponding pressure at the outlet of the evaporator is determined by

$$P_4 = P_{sat}(T_4 - 5). \tag{3}$$

The degree of superheat of Stream 4 at the inlet of the turbine is set as 5 °C.

Table 2 gives all the other parameters used in this model. To compare with the results of the composition-adjustable Kalina cycle, most of these parameters are chose as the same as Table 1 in Ref. [31].

The thermal efficiency of the ORC is defined as

$$\eta_{th} = \frac{W_t - W_{p1}}{Q_e} \times 100\%. \tag{4}$$

The exergy efficiency is calculated by

Table 2
Input parameters for the composition-adjustable ORC system.

Item	Parameter	Values
Heat source	Temperature T_{12}	100 °C
	Mass flow rate $\dot{m}_{water}$	141.8 kg/s
	Pressure P_{12}	2 MPa
Evaporator	Minimal pinch $\Delta T_{e,PPTD}$	5 K
	Maximum output temperature T_6	90 °C
Condenser	Minimal pinch $\Delta T_{c,PPTD}$	10 K
	Number of fans	40
	Power of fan	34 kW
	Air mass flow rate	120 kg/s per fan
Turbine	Isentropic efficiency η_t	0.85
Pump	Isentropic efficiency η_p	0.8

$$\eta_{ex} = \frac{W_t - W_{p1}}{dE} \times 100\%, \tag{5}$$

where dE is the exergy transferred from the geothermal brine to the zeotropic mixture in the evaporator. The mixer is assumed to be at static state. The detailed design of the mixer is beyond this paper. The power consumption of Pump 1 will increase slightly due to the resistance of the mixer. Hence, the power consumption of the mixer is ignored in this study.

As the working load of the turbine and the heat exchangers will vary as the ambient temperature changes, the ORC system may work at the off-design points. In this respect, the sizes of the turbine, the evaporator, the condenser, and the pump must be specified according to their maximum loads. In this analysis, a pinch-point analysis method is used for designing the evaporator and the condenser. Therefore, the heat transfer areas of these two heat exchangers are calculated according to the maximum values under various ambient temperatures. If the pinch-point temperature difference can satisfy with the working point with maximum heat load, it can also satisfy with the off-design points.

For the turbine, the calculated mass flow rate of the working fluid varies within a certain range (see Fig. 9(d)) and the turbine will work at off-design points when the ambient is too low or too high. Normally, the isentropic efficiency of a turbine drops under off-design conditions. However, the efficiency of the turbine is relatively insensitive to the offset from its design point in high-speed conditions and it can be assumed to operate with a constant isentropic efficiency via controlling the speed of the turbine [34]. As the power consumption of Pump 1 is very small, the change of power consumption when it operates under off-design points can be neglected in this study. Therefore, the above model can be used to analysis the performance when the system operates under off-design conditions.

A set of hourly sampled temperature data of Berlin in 2016 is used to simulate the changing ambient condition for the composition-adjustable ORC system. Fig. 6 shows three curves of the ambient temperature in different seasons. The solid line shows a typical temperature variation in a day of spring (or autumn), while the dashed and the dash-dotted lines are for winter and summer, respectively. It can be seen that the highest temperature reaches 31 °C in the summer while the lowest temperature reaches −1 °C in the winter. The daily temperature variation is smaller in the winter than other seasons.

According to the ambient conditions as described above, the required composition of the zeotropic mixture is calculated using the model. The corresponding thermal and exergy efficiencies of the ORC system are then computed. The composition corresponding to the maximum thermal efficiency is denoted as the optimal composition under the ambient temperature. In this way, the

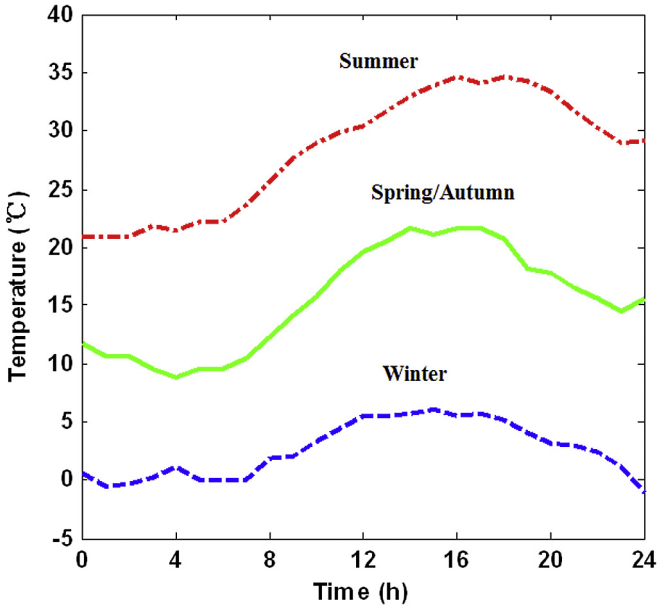

Fig. 6. Hourly temperature profiles in a day of different seasons in Berlin, Germany.

system performances of the composition-adjustable ORC can be obtained in different seasons.

The results are shown in Fig. 7. The net power output of the ORC system is shown in Fig. 7(a). In summer or spring/autumn, the net power output increases noticeably as the ambient temperature drops during the day. However, when the ambient temperature is below 0 °C, the system's net power output decreases slightly because the power consumption of the fans of the air-cooled condenser rises dramatically due to the decrease of the specific heat capacity of air. In general, the ambient temperature is higher in summer, so the mass fraction of R134a is lower (in a range of 0.07–0.24) as shown in Fig. 7(d). The system's thermal efficiency is also lower in the range of 7.29–8.53% as shown in Fig. 7(b). The mass fraction of R134 increases in spring/autumn as the ambient

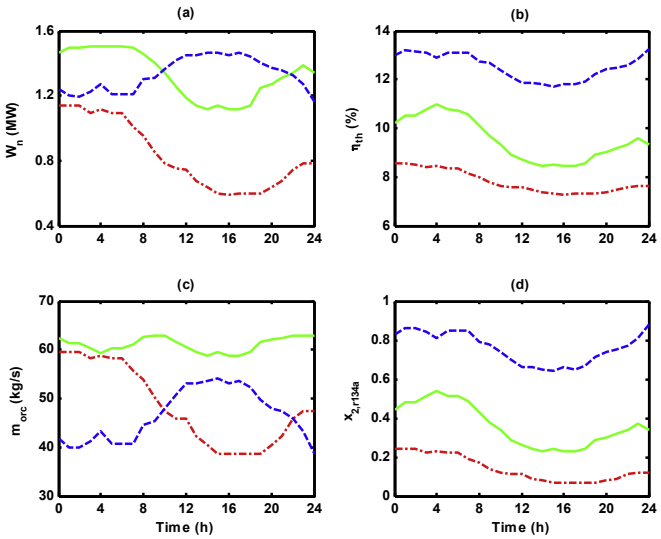

Fig. 7. Results as a function of time: (a) net power output (MW); (b) thermal efficiency (%); (c) mass flow rate of the zeotropic mixture (kg/s); (d) mass fraction of R134a of Stream 2. (The results in spring/autumn, summer, and winter are represented by the green solid lines, the red dash-dotted lines, and the blue dashed lines, respectively.)

temperature reduces. The system's thermal efficiency also rises noticeably. The ambient temperature decreases towards the minimum in winter, as a result, the mass fraction of R134a is adjusted to 0.64–0.88. Consequently, the system's thermal efficiency increases to the range of 11.7–13.28%. The mass flow of the working fluid mixture is shown in Fig. 7(c), which varies slowly when the ambient temperature is in the range of 10 and 20 °C. However, it decreases dramatically as the ambient temperature rises from 20 to 31 °C because the mass fraction of R245fa with a specific heat capacity greater than R134a increases rapidly. Therefore, the overall specific heat capacity of the zeotropic mixture also rises, leading to a decrease of the required mass flow rate of the zeotropic mixture in the evaporator since mass flow rate of geothermal brine is fixed for these simulations. On the other hand, the mass flow rate of the zeotropic mixture also decreases when the ambient temperature is below 10 °C because of a rapid increase of mass fraction of R134a having a smaller density.

Fig. 8(a) shows the thermal efficiency of the composition-adjustable ORC as a function of the ambient temperature and the mass fraction of R134a in Stream 1. Each solid line represents the thermal efficiency of the ORC as a function of the mass fraction of R134a for a given ambient temperature. It can be seen that the thermal efficiency of the ORC system increases as the mass fraction of R134a rises until an optimal value, and then decreases. Furthermore, as the ambient temperature decreases, the optimal mass fraction of R134a increases, while the corresponding maximum thermal efficiency increases. The optimal operation line (OOL) with maximum thermal efficiencies is obtained by connecting the optimal operating points for each given ambient temperature as shown by a dashed line in Fig. 8(a). It can be seen that the optimal thermal efficiency strongly depends on both the ambient temperature and the mass fraction of R134a. As shown in Fig. 8(b), the results of the exergy efficiency have a similar tendency. However, the exergy efficiency varies in a much narrower range than the thermal efficiency.

Fig. 8(c) shows the achievable maximum thermal efficiency of the proposed ORC system as a function of the ambient temperature. For comparison, the results of the composition-adjustable Kalina cycle using ammonia/water mixture as working fluid studied in reference [31] are also presented in Fig. 8 (c). It can be seen that the proposed ORC system can achieve higher thermal efficiencies than the composition-adjustable Kalina cycle [31] in the tested ambient temperature range. It is estimated that the annual average thermal efficiency of the former is around 20–30% higher than the latter according to the results shown in Fig. 8 (c). This can be attributed to the lower power consumption by the fans of the air-cooled condenser in the composition-adjustable ORC system studied in this research.

Similarly, the results of the corresponding conventional ORC cycle operating at a fixed composition temperature and condensation temperature based on the maximum summer ambient temperature are also shown in Fig. 8(c), which is expected to have an approximately constant thermal efficiency over the year. It can be seen that the proposed composition-adjustable ORC system can achieve significantly higher thermal efficiency than conventional ORC system as the ambient temperature decreases. According to the results shown in this figure, it is estimated that the annual average thermal efficiency of the composition-adjustable ORC is around 30–36% higher than its conventional counterpart. This agrees with the prediction using a simplified model in Ref. [30]. A comparative study with the composition tuning method is very complex if the condensation temperature of the conventional ORC or Kalina cycle using the zeotropic mixture also varies with the ambient temperature, which is beyond the scope of this paper.

Fig. 8 (d) shows the calculated maximum exergy efficiency of the

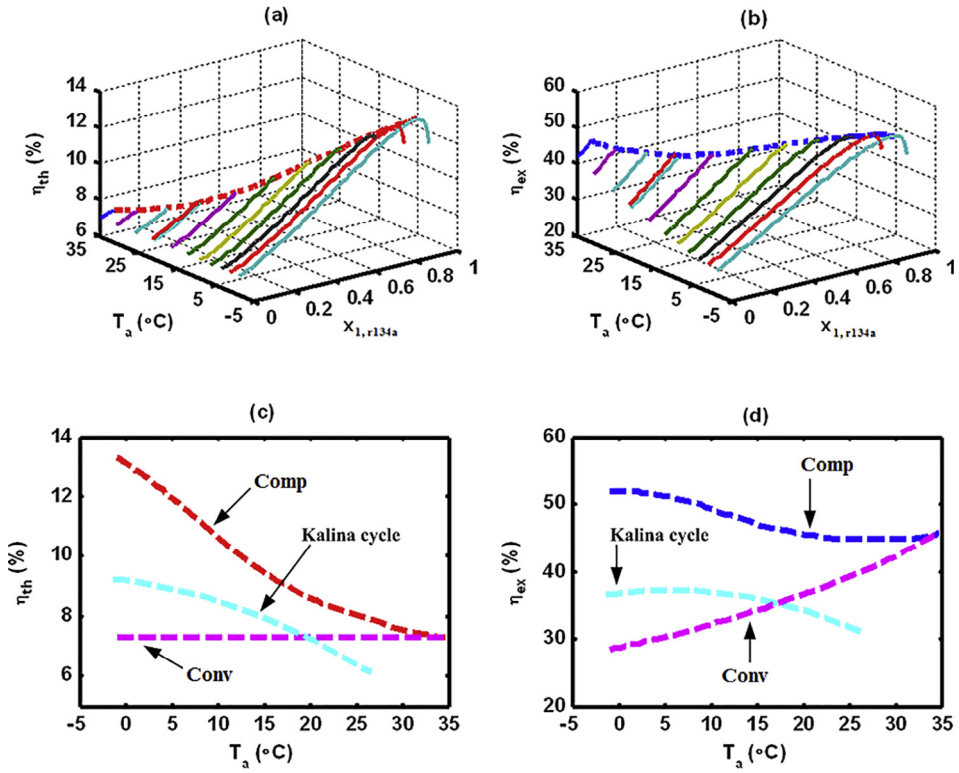

Fig. 8. Optimised results of thermal and exergy efficiencies as a function the mass fraction of R134a and ambient temperature. (Comp represents the composition-adjustable ORC cycle; Kalina cycle is the composition-adjustable Kalina cycle using ammonia/water as working fluid; Conv represents the conventional ORC.)

proposed system as a function of the ambient temperature. The exergy efficiency of the composition-adjustable ORC increases as the ambient temperature decrease. Similar to Fig. 8(c), the results of the composition-adjustable Kalina cycle using an ammonia/water mixture as working fluid [31] are also given in Fig. 8(d). Some investigations reported that the exergy efficiency of a Kalina cycle using ammonia/water is better than that of an ORC using R245fa [35], which agrees with our results when the ambient temperature is below around 20 °C as shown in Fig. 8(d). However, the tested Kalina cycle seems to have a lower thermal efficiency than a conventional ORC when the ambient temperature is above 20 °C. This is due to the fact that the ammonia mass fraction decreases dramatically when the ambient temperature is above 20 °C, leading to a decrease of net power output of the turbine.

Most conventional ORC systems are designed with a fixed condensation temperature/pressure. The condensation pressure is normally higher than the atmospheric pressure. Therefore, such a conventional ORC operating with a single working fluid has to be designed based on the maximum air temperature in summer to ensure the working fluid will be fully condensed in the condenser throughout the year. As the season shifts from summer to winter, the ambient temperature decreases. The working fluid in the condenser will potentially be subcooled due to the excessive cooling provided by the colder ambient air or water in winter. This will increase the heat input at the evaporator and reduce the cycle efficiency. To avoid such undesired subcooling, the flow rate of coolant passing the condenser normally needs to be reduced to keep the temperature of the working fluid close to the designed condensation temperature that is imposed by the condensing pressure. The power consumption of the fans of the air-cooled condenser reduces accordingly. On the other hand, because the temperature and the mass flow rate of the brine at the inlet of the evaporation is fixed in our analysis, the thermodynamic states and the mass flow rate of the working fluid inside the conventional ORC system is fixed, leading to a constant power output of the turbine. Normally, the power output of the turbine is significantly greater than the power consumption of the fans. Therefore, the change of the power consumption of the fans was negligible in this study and the net power output of the conventional ORC remains more or less constant as the ambient temperature changes. As the heat input to the evaporator remains constant, the thermal efficiency is approximately constant. However, because the “dead state” [36] for exergy calculation is based on the ambient temperature, the exergy of the geothermal heat source increases when the ambient temperature drops. Since the net power output keeps constant, the exergy efficiency of the conventional ORC decreases as the ambient temperature falls according to the second law of thermodynamics.

Fig. 9(a) presents the net power output of the composition-adjustable ORC system as a function of the ambient temperature. It increases and then decreases as the ambient temperature decreases, and reaches the maximum when the ambient temperature is 8.8 °C. Fig. 9(b) shows the relationship between the mass fraction of R134a in Stream 2 and the ambient temperature. The dynamic composition control strategy will adjust the mass fraction of R134a in Stream 2 based on this relationship when the ambient temperature varies. The corresponding density of Stream 2 is shown as a dome shape in Fig. 9(b) because the temperature of Stream 2 varies with the ambient temperature while its pressure remains constant.

Fig. 9(c) shows the calculated power production of the turbine, and the calculated power consumption of Pump 1 and the fans of the air-cooled condenser. The power consumption of the fans is calculated using the same method as Eq. (22) in Ref. [31]. The power consumption of the fans increases evidently as the ambient temperature drops because of the increment of the mass flow of the air, which is caused by the increase of the mass fraction of R134a. As the power of the turbine first increases and then decreases as the

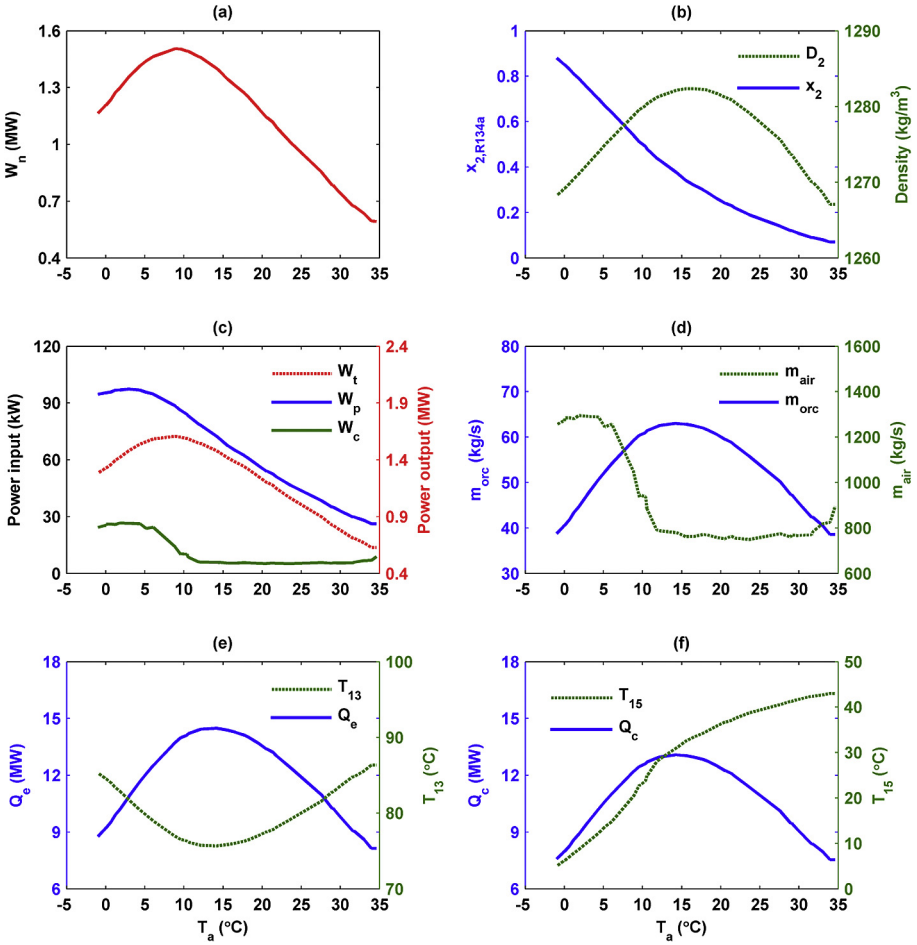

Fig. 9. Performance of the composition-adjustable ORC as a function of the ambient temperature: (a) net power output; (b) Mass fraction of R134a in Stream 2; (c) power consumption or output; (d) mass flow rates of the zeotropic mixture and the air in the condenser; (e) heat transfer in the evaporator and the geothermal water temperature at its outlet; (f) heat transfer in the condenser and the air temperature at its outlet.

ambient temperature decreases, the net power has a similar tendency. Fig. 9(d) presents the mass flow rates of the zeotropic mixture in the ORC system and the air passing the condenser. The mass flow rate of the working fluid in the ORC system firstly increases and then decreases as the ambient temperature decreases. The mass flow rate of air passing the condenser dramatically increases the ambient air temperature drops to below around 10 °C.

Fig. 9(e) shows the heat transfer in the evaporator and the temperature of the geothermal brine at the outlet of the evaporator. The heat transfer via the evaporator firstly increases and then decreases as the ambient air temperature decreases, which results from the variation of the mass flow rate of the working fluid in the ORC system as shown in Fig. 9(d). Consequently, the temperature of the geothermal brine exiting the evaporator firstly decreases and then increases as the ambient temperature decreases.

Essentially, as the ambient temperature decreases, the corresponding temperature at the inlet of the evaporator also decreases. However, the mass fraction of R134a and the pressure of the zeotropic mixture in the evaporator increases. Using the pinch point analysis method, the variation tendency of the temperature of the brine at the outlet of the evaporator is obtained. Because the boundary conditions listed in Table 2 set the temperature and the mass flow of the brine constant, the heat transfer in the evaporator shows an inverse trend.

Fig. 9(f) presents the heat transfer in the condenser and the air temperature at the outlet of the evaporator. As the ambient temperature increases, the outlet air temperature increases accordingly. However, the heat transfer via the condenser firstly increases and then decreases as the ambient air temperature increases. This can be attributed to the change of load as shown in Fig. 9(e).

4. Dynamic composition control strategy

The composition-adjustable ORC needs to regulate the composition of the zeotropic mixture when the ambient temperature changes. Therefore, a dynamic composition control strategy based on an optimisation algorithm is proposed in this section. It is assumed that the amount of the zeotropic working fluid can be circulated around the ORC system in 5 min. In this study, this value is specified based on the charge of working fluid in the main ORC [30] and the mass flow rate of Pump 1. It is assumed that the entire charge can be circulated completely within this time interval. Normally, the transient processes of an ORC take several minutes [37,38]. It may be not enough for the main ORC to be stabilized within 5 min because of the thermal inertia of the heat exchangers. However, if the composition of the zeotropic mixture can be tuned to follow the optimal value based on the ambient temperature, it will be beneficial for the control of Pump 1 and the fans of the condenser. In practice, the updated frequency of the zeotropic mixture is determined by the bulk volume of the working fluid inside the main ORC circuit and the mass flow rate of Pump 1. The

sample frequency of the distillation system should take into account this updated frequency and the variation characteristics of the ambient temperature. The composition control strategy can sample the ambient temperature and control the mass flow rates in a step of every 5 min. First, the required mass fraction of R134a in Stream 2 is optimised according to the ambient temperature as described in the above sections. In the mixer, the mass and composition balances can be represented by

$$m_{10}(i) + m_{11}(i) - m_6(i) = m_2(i+1) - m_2(i), \tag{6}$$

$$\alpha_1 m_{10}(i) + \alpha_2 m_{11}(i) - x_2(i) m_6(i) = x_2(i+1) m_2(i+1) - x_2(i) m_2(i), \tag{7}$$

where $m_j(i)$ is the mass flow rate of stream j at the sample time i, x_2 is the mass fraction of R134a in Stream 2, α_1 is the mass fraction of R134a in Stream 10 (i.e., 0.98), and α_2 is the mass fraction of R134a in Stream 11 (i.e., 0.02). Both the required mass flow rate and the mass fraction of R134a of Stream 2 are input variables.

The main ORC system is already optimised and assumed to operate along the OOL line shown in Fig. 8 in the above section. The purpose of this study is to investigate the dynamic control strategy of its subsystem, i.e., the composition tuning subsystem. Firstly, we need to determine the corresponding mass flow rates of Streams 6, 10, and 11, respectively, so that the main ORC system can operate along the OOL line. In this section, an optimisation algorithm has been developed and the objective is to minimize the total mass flow rates of Streams 6, 10, and 11.

$$min: \quad m_6(i) + m_{10}(i) + m_{11}(i) \tag{8}$$

The boundary conditions are that the mass flow rates of these three streams must not be negative.

$$m_6(i) \geq 0 \tag{9}$$

$$m_{10}(i) \geq 0 \tag{10}$$

$$m_{11}(i) \geq 0 \tag{11}$$

This optimisation algorithm can be solved by a linear programme method and the solution is given by

$$m_6(i) = max\left(0, \quad \frac{\Delta M - \alpha_1 \Delta m}{\alpha_1 - x_2(i)}, \quad \frac{\alpha_2 \Delta m - \Delta M}{x_2(i) - \alpha_2}\right), \tag{12}$$

$$m_{10}(i) = \frac{\Delta M - \alpha_2 \Delta m + m_6(i)(x_2(i) - \alpha_2)}{\alpha_1 - \alpha_2}, \tag{13}$$

$$m_{11}(i) = \frac{\alpha_1 \Delta m - \Delta M + m_6(i)(\alpha_1 - x_2(i))}{\alpha_1 - \alpha_2}, \tag{14}$$

where $\Delta m = m_2(i+1) - m_2(i)$, $\Delta M = x_2(i+1) m_2(i+1) - x_2(i) m_2(i)$.

Based on this dynamic composition control strategy, the results of the mass flow rates of Streams 6, 10, and 11 are calculated and shown in Fig. 10 when the ambient temperature in the autumn/spring is used as the input data. Fig. 11 shows the mass flow rates for the summer and the winter cases. It can be seen that all the mass flow rates of Streams 6, 10, and 11 are less than 3 kg/s, which are much lower than the mass flow rate of working fluid in the ORC system (around 40–50 kg/s) as shown in Fig. 7(c). The dynamic composition control strategy increases the mass flow rate of Stream 10 if the ambient temperature drops. Otherwise, the mass flow rate of Stream 11 is increased. The mass flow rate of Stream 6 extracted from the ORC system is used to balance the composition of Stream 2. In most of the cases, only stream 10 is added when the concentration of R134a in Stream 2 needs to be enriched and only stream 11 is pumped to decrease the mass fraction of R134a.

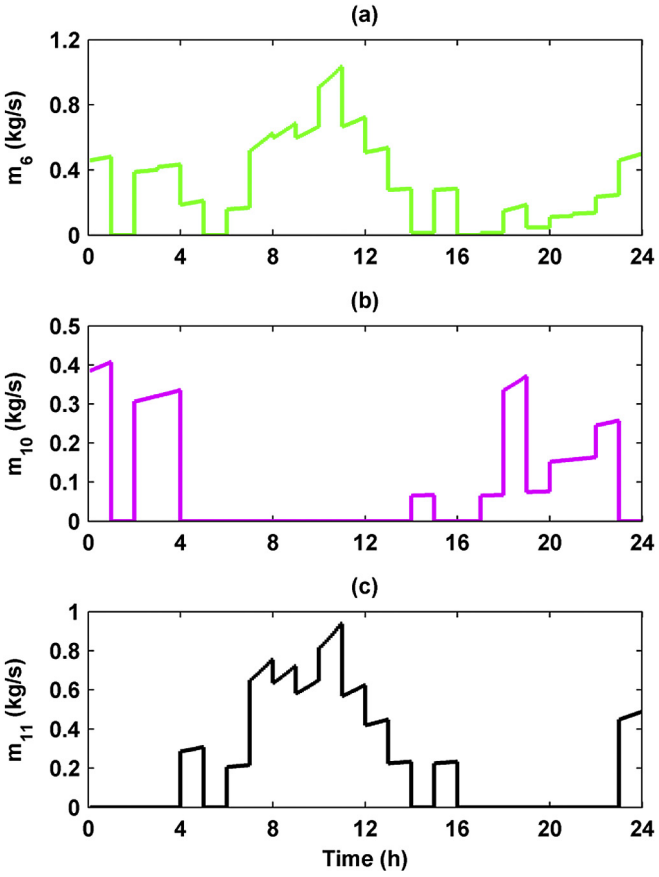

Fig. 10. Optimised mass flow rates of the distillation column at the inlet and outlets for the spring/autumn case.

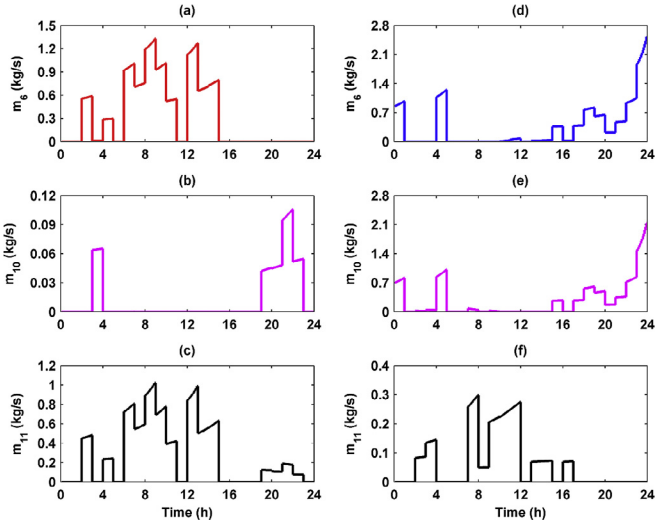

Fig. 11. Optimised mass flow rates of the distillation column for the summer and winter cases. (The results of (a), (b), and (c) are for the summer case; the results of (d), (e), and (f) are for the winter case.).

5. Dynamic response characteristics

5.1. Design of distillation column

The results obtained by the dynamic composition control strategy show that the mass flow rate of Stream 6 changes abruptly with time. However, the distillation process in the distillation column takes time. Therefore, Steam 6 is not suitable to be directly fed to the distillation column. Instead, Tank 2 is added at the inlet of the distillation column to buffer the fluctuation of Stream 6. Tanks 3 and 4 are also added at the outlets of the distillation column to store the separated components temporarily. In this study, it is assumed that Tank 2 stores the mixture from Stream 6 for a whole day and an average mass flow is pumped to the distillation column at the next day. In this way, the mass flow rate into the distillation column can be kept stable during a day and it is very helpful for the steady operation and size reduction of the distillation column. Based on the results of Figs. 10 and 11, the daily average mass flow into the column is calculated as 0.309 kg/s for the spring/autumn cases and the corresponding mass fraction of R134a is 0.366. In the summer, the daily average mass flow rate is calculated as 0.332 kg/s and the corresponding mass fraction is decreased to 0.145. In the winter, the daily average mass flow rate is obtained as 0.339 kg/s and the corresponding mass fraction is increased to 0.783. To keep a certain margin for the column design, the maximum mass flow is selected as 0.44 kg/s.

Using the above data as an input, the main parameters of the distillation column are designed using Aspen Plus V8.8 software. The steady state model is shown in Fig. 12. This model has been validated using a zeotropic mixture of propane/isobutene with the model in Ref. [39] and the steady errors are less than 1.5%. Afterwards, the working fluid is replaced with R134a/R245fa which is used in this research. The input parameters of the Aspen model are listed in Table 3. The purities of the two streams at the outlets of the distillation column are set as 0.98 for this analysis. The number of trays of the column is set to be 16 after several attempts. The mixture flows into the distillation column at the 8th tray. The height of each tray is specified as 0.25 m. The calculated diameters of the column are 0.38, 0.34, and 0.39 m for the cases in spring/autumn, the summer, and the winter, respectively. Therefore, the final diameter of the column is set as 0.38 m. Then, the operation performance of the distillation column in different seasons is evaluated and shown in Table 4. It can be seen that the required purities are satisfactory for both streams at the outlets of the distillation column. The operational parameters inside the distillation column are shown in Fig. 13 when the ambient temperature in spring/autumn is used as an example. The tray at the top of the column is numbered as no. 1, so the tray at the bottom is numbered as no. 16. The working temperature and pressure of the zeotropic mixture rises gradually as the stage increases while the mass fractions of R134a in the gaseous and liquid fluids are both decreased.

The energy consumption of the reboiler and the condenser of the distillation system are shown in Table 5. The heat consumption of the reboiler is always below 130 kW under all tested conditions, which is around 1% of the heat input to the evaporator (i.e. around 9–15 MW) of the main ORC system. The results of the power consumption of the pumps of the distillation system are listed in Table 6. Compared with the power consumption of the main ORC, the corresponding power input are negligible because the mass flow rates of these pumps are very small. For the Pumps 2, 4, and 5, the values are the maximum power consumption corresponding to the results of Figs. 10 and 11. In Aspen Plus environment, the model of the condenser of the distillation column is cooled by water and only the heat duty can be obtained. If an air-cooled condenser is used for the distillation column, the power consumption of the condenser can be evaluated using the same method as the air-cooled condenser of the main ORC. The cost of the distillation system has been discussed in reference [30]. Therefore, in this study, we only focus the thermodynamic performance of the distillation system.

Table 3
Input parameters for the Aspen model.

Component	Parameter	Value
Pump 2	Output pressure	0.8 MPa
Pump 3	Output pressure	1.8 MPa
	Number of stages	16
Distillation column	Feed stage	8
	Stage pressure drop	680 Pa
	Column diameter	0.38 m
	Tray height	0.25 m
Valve 1	Pressure drop	0.3 MPa
Valve 2	Pressure drop	0.3 MPa
Pump 4	Output pressure	1.5 MPa
Pump 5	Output pressure	1.5 MPa

Tanks 2, 3 and 4 are used to buffer the mass flows into and out from the distillation column. The volumes of Tanks 2, 3, and 4 must be evaluated based on all seasons. According to the results in Section 5.2, the response time of the distillation column is less than 6 h. If the mass flow rate of Pump 3 updates every 6 h, the volumes of these tanks can be less than 5.5 m^3. On the other hand, similar to reference [30], if the charge of working fluid is set to 6000 kg, which only takes up about 4.8 m^3 in liquid form. If all the working fluid in the main ORC is changed from R134a to R245fa, the required volumes for Tanks 2, 3, and 4 are also less than 5.5 m^3. In practice, the volumes of the tanks need to be specified according to the buffered bulk mass and the charge in the main ORC.

5.2. Dynamic performance of distillation column

The mass flow rate entering into the distillation column can be kept steady within a day according to the dynamic composition control strategy. However, the ambient temperature differs between any two continuous days. Therefore, it is necessary to analyse the dynamic response of the distillation subsystem when the ambient temperature varies day-to-day. In this study, two extreme

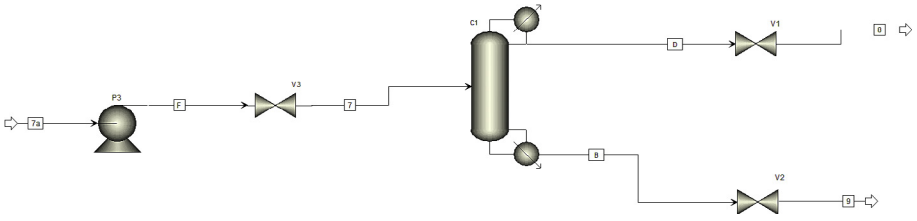

Fig. 12. Steady state model of the distillation column in Aspen Plus.

Table 4
Results of the distillation column.

Parameter	Spring/Autumn			Summer			Winter		
	Str 7	Str 8a	Str 9a	Str 7	Str 8a	Str 9a	Str 7	Str 8a	Str 9a
Temperature (°C)	28.7	52.0	102.3	40.7	52.0	102.3	14.7	52.0	102.3
Pressure (MPa)	1.5	1.37	1.38	1.5	1.37	1.38	1.5	1.37	1.38
Mass flow (kg/s): R134a	0.1612	0.1555	0.0056	0.0636	0.0559	0.0077	0.3444	0.3426	0.0018
Mass flow (kg/s): R245fa	0.2788	0.0032	0.2757	0.3764	0.0011	0.3753	0.0956	0.0070	0.0886
Mass fraction: R134a	0.366	0.98	0.02	0.145	0.98	0.02	0.783	0.98	0.02
Mass fraction: R245fa	0.634	0.02	0.98	0.856	0.02	0.98	0.217	0.02	0.98
Vapor fraction	0	0	0	0	0	0	0	0	0
Liquid fraction	1	1	1	1	1	1	1	1	1
Total flow (kg/s)	0.440	0.159	0.281	0.440	0.0571	0.383	0.440	0.350	0.090

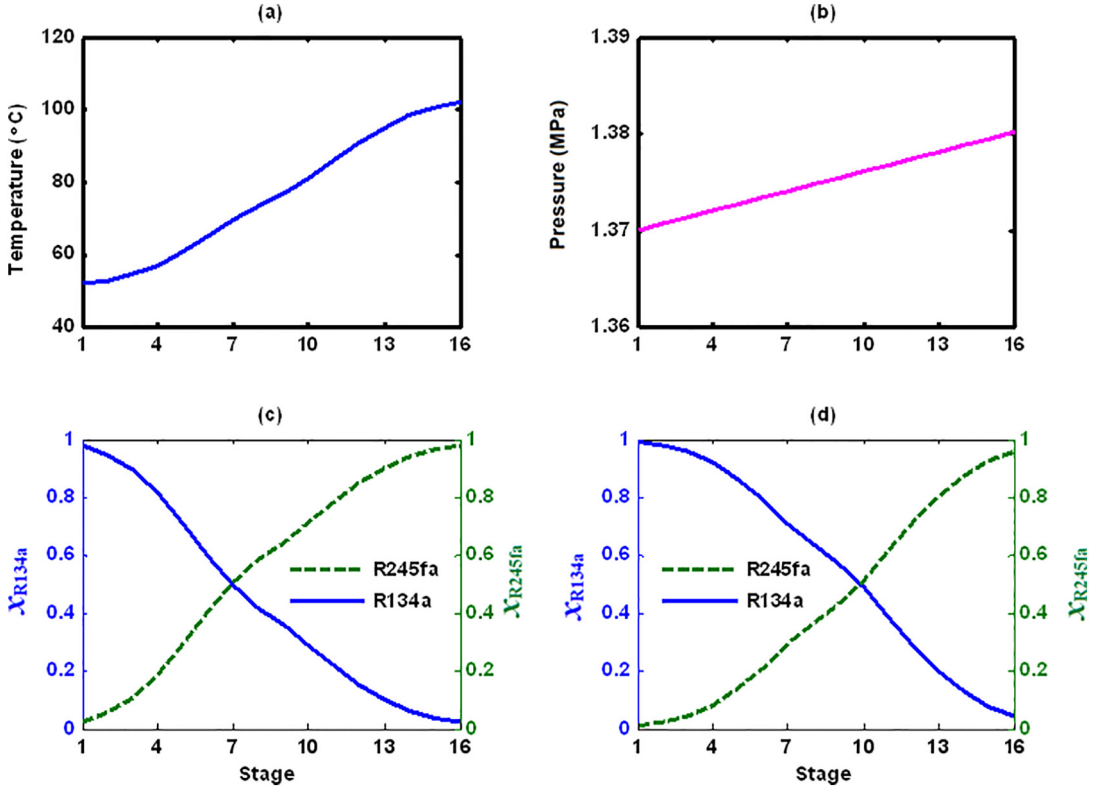

Fig. 13. Steady state simulation results of the distillation column for the spring/autumn case: (a) operation temperature as a function of the tray number in the distillation column; (b) operation pressure; (c) component mass fraction of the liquid mixture; (d) component mass fraction of the gaseous mixture.

Table 5
Results of the condenser and the reboiler of the distillation system.

	Parameter	Spring/Autumn	Summer	Winter
Condenser	Temperature (°C)	52	52	52
	Heat duty (kW)	84.66	60.99	98.6
	Distillate rate (kg/s)	0.1587	0.0571	0.3496
	Reflux rate (kg/s)	0.3910	0.3389	0.2906
	Reflux ratio	2.463	5.939	0.831
Reboiler	Temperature (°C)	102.3	102.3	102.3
	Heat duty (kW)	120.9	97.3	129.9
	Bottoms rate (kg/s)	0.2813	0.3829	0.0904
	Boilup rate (kg/s)	0.8874	0.7138	0.9531
	Boilup ratio	3.155	1.864	10.539

situations are specified: Case 1 assumes the ambient temperature changes from a day in spring/autumn to a day in summer. Case 2 assumes the temperature transits from a day in spring/autumn to a day in winter.

Table 6
Power consumption for the pumps of the distillation system (kW).

	Spring/Autumn	Summer	Winter
Pump 2	1.08	1.40	2.66
Pump 3	0.82	0.88	0.89
Pump 4	0.54	0.14	2.90
Pump 5	1.24	1.35	0.40

A dynamic model of the distillation column is established using Aspen Plus Dynamics to analyse the system response characteristics in these two extreme scenarios. Fig. 14 shows the dynamic model including the control system. The dynamic model of the distillation column is validated using a zeotropic mixture of propane/isobutane as shown in Ref. [39] and the maximum difference of the response time is less than 3 min. Then, the working fluid is changed to R134a/R245fa and all the control parameters are recalibrated. The controller of the distillation column is a multi-input

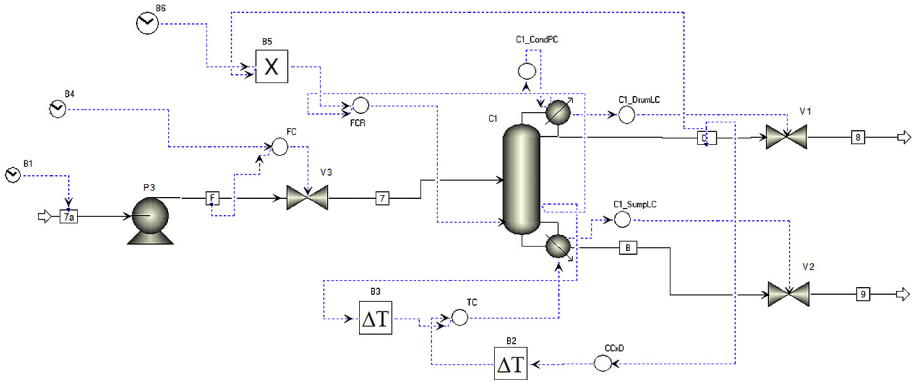

Fig. 14. Dynamic model of the distillation column in Aspen Plus Dynamics.

and multi-output control system and it can be decoupled to four main single-input and single-output controllers shown in Fig. 14. The controller C1_DrumLC regulates the opening of Valve 1 proportionally according to the required liquid level of the reflux drum of the condenser. Similarly, the controller C1_SumpLC controls the liquid level of the reboiler sump by adjusting the opening of Valve 2. The proportional-integral (PI) controller C1_CondPC controls the operation pressure of the condenser of the distillation system by manipulating the heat removal of the condenser. The last controller is a cascade controller consisting of TC and CCxD. The inner PI controller TC regulates the heat power of the reboiler according to the working temperature of the 9th stage. The target value of the TC controller is configured by the outer CCxD controller, of which the input variable is the mass fraction of R245fa in Stream 8. The CCxD controller also uses a PI control algorithm. Considering the time delays of the temperature and density sensors, two delay blocks are inserted into the dynamic model.

The results of Case 1 are shown in Fig. 15. The profile of the mass flow rate of the mixture entering into the distillation column is shown in Fig. 15(a), and it is stepped from 0.309 to 0.332 kg/s at the second hour. The variation of the corresponding mass fraction of R134a is shown in Fig. 15(b), and its concentration decreases from 0.366 to 0.145. These two profiles are used as input data for the dynamic model. The mass flow rates of Streams 8 and 9 are shown in Fig. 15(c) and (d), respectively. Because the mass flow rate into the distillation column only increases slightly but the mass fraction of R134a decreases significantly, the mass flow rate of Stream 8 rich in R134a decreases from 0.111 to 0.044 kg/s, while the mass flow of Stream 9 increases from 0.197 to 0.288 kg/s. The impurities of Streams 8 and 9 fluctuates during the dynamic process shown as Fig. 15(e) and (f). The required heat input to the reboiler is shown in Fig. 15(g) and it changes from 84.6 to 80.0 kW. The heat rejection in the condenser of the distillation system decreases from 59.4 to 47.4 kW as shown in Fig. 15(h). It can be seen that the output impurities of the distillation column can satisfy the requirements during the dynamic process and the response time of the distillation column is less than 4 h.

The results of Case 2 are shown in Fig. 16. In this case, the mass flow rate of mixture into the column changes from 0.309 to 0.339 kg/s while the mass fraction of R134a steps dramatically from

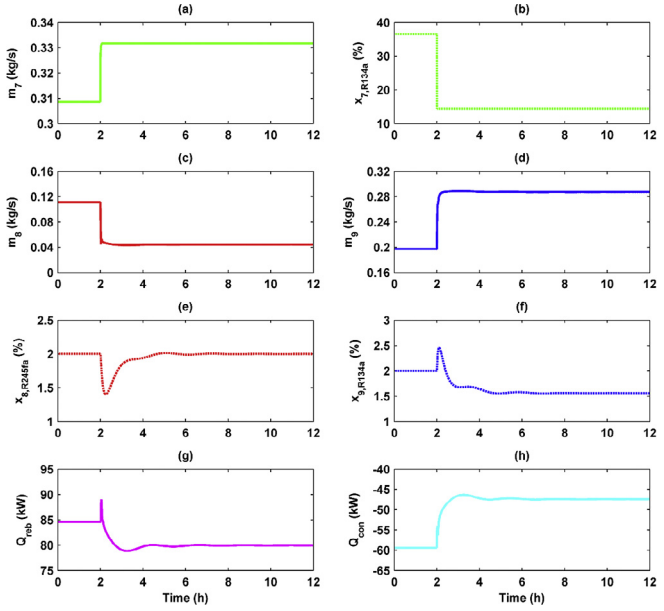

Fig. 15. Results of dynamic process when the ambient temperature rises from the spring/autumn to the summer: (a) mass flow rate of Stream 7; (b) mass fraction of R134a in Stream 7; (c) mass flow rate of Stream 8; (d) mass flow rate of Stream 9; (e) mass fraction of R245fa in Stream 8; (f) mass fraction of R134a in Stream 9; (g) heat addition of the reboiler; (h) heat rejection via the condenser of the distillation system.

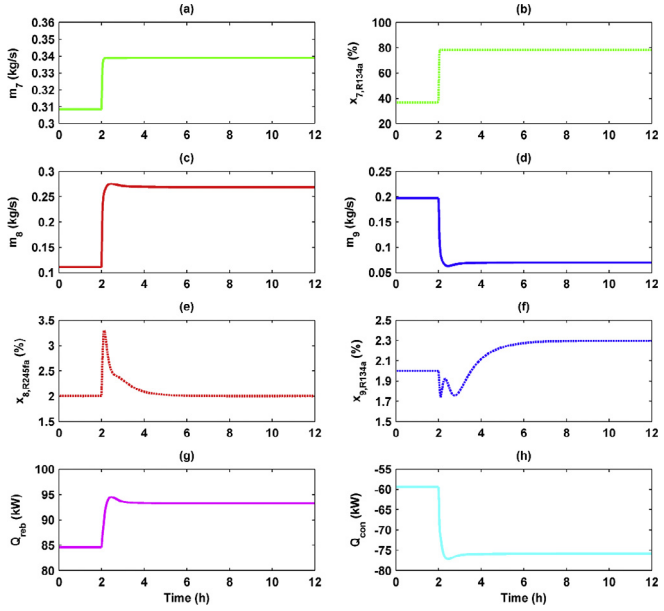

Fig. 16. Results of dynamic process when the ambient temperature drops from the spring/autumn to the winter: (a) mass flow rate of Stream 7; (b) mass fraction of R134a in Stream 7; (c) mass flow rate of Stream 8; (d) mass flow rate of Stream 9; (e) mass fraction of R245fa in Stream 8; (f) mass fraction of R134a in Stream 9; (g) heat addition of the reboiler; (h) heat rejection via the condenser of the distillation system.

0.366 to 0.783. The results show an opposite variation tendency for each of the working parameters. The impurities of Streams 8 and 9 are slightly greater than 2% but it does not have a great effect on the system performance. The response time of Case 2 is a bit larger than Case 1 but it is still less than 6 h due to a larger magnitude of variation in the mass fraction of R134a shown in Fig. 16(b).

It should be noted that these cases are two worst-case scenarios. In reality, the ambient air temperature does not change dramatically. Hence, the required adjustment of composition will be much less than two envisaged cases above. Furthermore, we will only need to adjust the composition once per day to match ORC system with the average ambient temperature in either daytime or nigh time as shown in Fig. 6. Therefore, the response time of the designed distillation system is short enough to satisfy the requirement.

Investigations indicated that the dynamic response time of an ORC is normally from several minutes to over 10 min [37,38]. If the distillation column is connected with the main ORC without Tanks 2, 3, and 4, the purities of Streams 10 and 11 cannot satisfy the real-time requirements because the response time of the distillation column is a couple of hours, which is verified by the dynamic model in the Aspen Plus Dynamics. Therefore, Tanks 2, 3, and 4 together with Pumps 2, 4, and 5 are added. In this way, the dynamic control of the distillation system can be decoupled from the main ORC. The input of the distillation is updated in a very long-time interval (24 h in this study) and the outputs of the distillation can always maintain at a high level of purity. On the other hand, the ambient temperature normally does not change significantly in half an hour. Accordingly, the composition of mixture varies relatively slowly. Since the mass fraction of the mixed working fluid changes, the evaporation pressure and the superheat degree may change during the transient process of the main ORC. Therefore, the optimised results of the mass flow rates may be different from that shown in Figs. 10 and 11. However, we can use the same method presented in Sections 3 and 4 to determine these mass flow rates in real-time applications. Tanks 2, 3, and 4 can buffer these variations. Furthermore, the results in this section indicate that the dynamic performance of the distillation system can satisfy with the extreme variations of the ambient temperature from spring/autumn to summer or winter. Therefore, it is feasible for the designed dynamic control strategy of the distillation system to follow the requirements of the composition change caused by the transient process of the main ORC when the ambient temperature changes.

6. Conclusions

In this paper, a dynamic composition control strategy has been proposed and analysed for a composition-adjustable ORC system using zeotropic mixture as working fluid. This method employs a distillation column to separate the two components of the mixture. One of the obtained component fluids will then be pumped back to the main ORC system to adjust the composition of the zeotropic mixture to the required level according to the ambient temperature. The dynamic composition control strategy is simulated using an optimisation algorithm. The design method of the distillation column is presented and the dynamic response characteristics of the distillation column has been analysed. The main conclusions are summarised as follows:

1) As the temperature glide of the zeotropic mixture consisting of R245fa and R134a is too small to use a separator separate them like Kalina cycle, a distillation column is proposed to separate the mixture. The obtained high purity R245fa and R134a can then be used to regulate the composition of the zeotropic mixture in the main ORC system. The results indicate that it is a suitable method for control the composition of this ORC system.
2) For power generation from low-temperature geothermal sources, a composition-adjustable ORC with zeotropic mixture can reduce the losses in the condenser and improve the system thermal efficiency as well as net power output significantly. Comparing with a conventional ORC system, the annual average system thermal efficiency can be significantly increased as the ambient temperature decreases when the season changes from summer to winter.
3) The simulation results of the composition-adjustable ORC have also been compared with a composition-adjustable Kalina cycle using ammonia/water as working fluid. The research shows that the former can potentially be 20–30% more efficient than the latter, showing that the composition-adjustable ORC using a zeotropic mixture of R245fa/R134a as working fluid has great potential for efficient power generation from low temperature geothermal energy sources.
4) The proposed dynamic composition control strategy can regulate the composition of the zeotropic mixture of the main stream according to the ambient temperature. The mass flow rate extracted to the distillation column is far less than that of the main stream of the ORC system. Therefore, the size and energy consumption of the distillation column are relatively small. The extra heat consumption by the distillation column is only around 1% of the heat input to the ORC system.
5) The designed distillation column can separate the zeotropic mixture during the dynamic control process when the ambient temperature varies from day to day and the purities can be controlled at around 98%. The dynamic response time of the distillation column increases as the difference of the day-to-day ambient temperature variation increases. The required response time is in the range of 4–6 h for envisaged worst-case of scenario. The actual required response time will be much less. Furthermore, considering only composition adjustment will be required for each day, the dynamic performance of distillation system can satisfy the requirements.

Acknowledgements

This research is funded by EPSRC (Ref: EP/N005228/1 and EP/N020472/1) and Royal Society (Ref: IE150866) in the UK.

Nomenclature

dE	exergy transferred from brine (kJ)
P	pressure (MPa)
Q	heat quantity (kW)
T	temperature (K)
W	power (kW)
m	mass flow rate (kg/s)
x	mass fraction

Greek letters

α_1	mass fraction of R134a in Stream 10
α_2	mass fraction of R134a in Stream 11
η	efficiency

Subscript

a	ambient condition
e	evaporator
ex	exergy efficiency
hs	heat source
$p1$	Pump 1
sat	saturation

t	Turbine
th	thermal efficiency

Acronyms

HC	hydrocarbon
HFC	hydrofluorocarbon
HFO	hydrofluoroolefins
OOL	optimal operation line
ORC	organic Rankine cycle
PI	proportional-integral
PPTD	pinch point temperature difference

References

[1] Zhu J, Hu K, Lu X, Huang X, Liu K, Wu X. A review of geothermal energy resources, development, and applications in China: current status and prospects. Energy 2015;93:466–83.
[2] Eyidogan M, Kilic FC, Kaya D, Coban V, Cagman S. Investigation of organic Rankine cycle (ORC) technologies in Turkey from the technical and economic point of view. Renew Sustain Energy Rev 2016;58:885–95.
[3] Bao J, Zhao L. A review of working fluid and expander selections for organic Rankine cycle. Renew Sustain Energy Rev 2013;24:325–42.
[4] Angelino G, Colonna Di Paliano P. Multicomponent working fluids for organic Rankine cycles (ORCs). Energy 1998;23:449–63.
[5] Habka M, Ajib S. Evaluation of mixtures performances in Organic Rankine Cycle when utilizing the geothermal water with and without cogeneration. Appl Energy 2015;154:567–76.
[6] Kang Z, Zhu J, Lu X, Li T, Wu X. Parametric optimization and performance analysis of zeotropic mixtures for an organic Rankine cycle driven by low-medium temperature geothermal fluids. Appl Therm Eng 2015;89:323–31.
[7] Radulovic J, Castaneda NIB. On the potential of zeotropic mixtures in supercritical ORC powered by geothermal energy source. Energy Convers Manag 2014;88:365–71.
[8] Yang K, Zhang H, Wang Z, Zhang J, Yang F, Wang E, et al. Study of zeotropic mixtures of ORC (organic Rankine cycle) under engine various operating conditions. Energy 2013;58:494–510.
[9] Li YR, Du MT, Wu CM, Wu SY, Liu C. Potential of organic Rankine cycle using zeotropic mixtures as working fluids for waste heat recovery. Energy 2014;77:509–19.
[10] Chaitanya Prasad GS, Suresh Kumar C, Srinivasa Murthy S, Venkatarathnam G. Performance of an organic Rankine cycle with multicomponent mixtures. Energy 2015;88:690–6.
[11] Vivian J, Manente G, Lazzaretto A. A general framework to select working fluid and configuration of ORCs for low-to-medium temperature heat sources. Appl Energy 2015;156:727–46.
[12] Zhao L, Bao J. Thermodynamic analysis of organic Rankine cycle using zeotropic mixtures. Appl Energy 2014;130:748–56.
[13] Chys M, van den Broek M, Vanslambrouck B, De Paepe M. Potential of zeotropic mixtures as working fluids in organic Rankine cycles. Energy 2012;44:623–32.
[14] Hærvig J, Sørensen K, Condra TJ. Guidelines for optimal selection of working fluid for an organic Rankine cycle in relation to waste heat recovery. Energy 2016;96:592–602.
[15] Basaran A, Ozgener L. Investigation of the effect of different refrigerants on performances of binary geothermal power plants. Energy Convers Manag 2013;76:483–98.
[16] Aghahosseini S, Dincer I. Comparative performance analysis of low-temperature Organic Rankine Cycle (ORC) using pure and zeotropic working fluids. Appl Therm Eng 2013;54:35–42.
[17] Desideri U, Bidini G. Study of possible optimisation criteria for geothermal power plants. Energy Convers Manag 1997;38:1681–91.
[18] Yue C, Han D, Pu W, He W. Thermal matching performance of a geothermal ORC system using zeotropic working fluids. Renew Energy 2015;80:746–54.
[19] Heberle F, Preißinger M, Brüggemann D. Zeotropic mixtures as working fluids in Organic Rankine Cycles for low-enthalpy geothermal resources. Renew Energy 2012;37:364–70.
[20] Liu Q, Shen A, Duan Y. Parametric optimization and performance analyses of geothermal organic Rankine cycles using R600a/R601a mixtures as working fluids. Appl Energy 2015;148:410–20.
[21] Andreasen JG, Larsen U, Knudsen T, Haglind F. Design and optimization of a novel organic Rankine cycle with improved boiling process. Energy 2015;91:48–59.
[22] Liu Q, Duan Y, Yang Z. Effect of condensation temperature glide on the performance of organic Rankine cycles with zeotropic mixture working fluids. Appl Energy 2014;115:394–404.
[23] Li J, Liu Q, Duan Y, Yang Z. Performance analysis of organic Rankine cycles using R600/R601a mixtures with liquid-separated condensation. Appl Energy 2017;190:376–89.
[24] Imran M, Usman M, Park BS, Yang Y. Comparative assessment of Organic Rankine Cycle integration for low temperature geothermal heat source applications. Energy 2016;102:473–90.
[25] Mavrou P, Papadopoulos AI, Seferlis P, Linke P, Voutetakis S. Selection of working fluid mixtures for flexible Organic Rankine Cycles under operating variability through a systematic nonlinear sensitivity analysis approach. Appl Therm Eng 2015;89:1054–67.
[26] Victor RA, Kim JK, Smith R. Composition optimisation of working fluids for organic rankine cycles and Kalina cycles. Energy 2013;55:114–26.
[27] Li T, Zhang Z, Lu J, Yang J, Hu Y. Two-stage evaporation strategy to improve system performance for organic Rankine cycle. Appl Energy 2015;150:323–34.
[28] Sadeghi M, Nemati A, Ghavimi A, Yari M. Thermodynamic analysis and multi-objective optimization of various ORC (organic Rankine cycle) configurations using zeotropic mixtures. Energy 2016;109:791–802.
[29] Thierry DM, Flores-Tlacuahuac A, Grossmann IE. Simultaneous optimal design of multi-stage organic Rankine cycles and working fluid mixtures for low-temperature heat sources. Comput Chem Eng 2016;89:106–26.
[30] Collings P, Yu Z, Wang E. A dynamic organic Rankine cycle using a zeotropic mixture as the working fluid with composition tuning to match changing ambient conditions. Appl Energy 2016;171:581–91.
[31] Wang E, Yu Z. A numerical analysis of a composition-adjustable Kalina cycle power plant for power generation from low-temperature geothermal sources. Appl Energy 2016;180:834–48.
[32] Abadi GB, Yun E, Kim KC. Experimental study of a 1 kw organic Rankine cycle with a zeotropic mixture of R245fa/R134a. Energy 2015;93:2363–73.
[33] Gorak A, Sorensen E. Distillation: fundamentals and principles. London: Academic Press; 2014.
[34] Pierobon L, Nguyen TV, Mazzucco A, Larsen U, Haglind F. Part-load performance of a wet indirectly-fired gas turbine integrated with an Organic Rankine Cycle turbogenerator. Energies 2014;7:8294–316.
[35] Mergner H, Weimer T. Performance of ammonia-water based cycles for power generation from low enthalpy heat sources. Energy 2015;88:93–100.
[36] Cengel YA, Boles MA. Thermodynamics – an engineering approach. sixth ed. London: McGraw-Hill; 2008.
[37] Quoilin S, Aumann R, Grill A, Schuster A, Lemort V. Dynamic modelling and optimal control strategy of waste heat recovery organic Rankine cycles. Appl Energy 2011;88:2183–90.
[38] Hou G, Bi S, Lin M, Zhang J, Xu J. Minimum variance control of organic Rankine cycle based waste heat recovery. Energy Convers Manag 2014;86:576–86.
[39] Luyben WL. Distillation design and control using Aspen™ simulation. second ed. Hoboken, New Jersey: John Wiley & Sons; 2013.